MECHANICAL

TECHNOLOGY

INCORPORATED

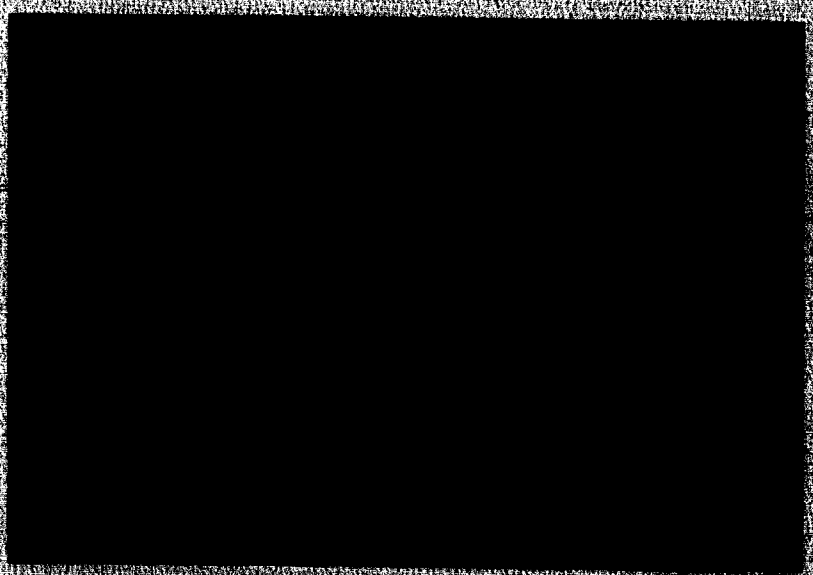

MECHANICAL TECHNOLOGY INCORPORATED
968 Albany-Shaker Road
Latham, New York 12110

MTI-66TR7

ON THE SLOWLY TIME DEPENDENT PROBLEM OF SQUEEZE FILM BEARINGS

by

C.H.T. Pan
T. Chiang
H.G. Elrod, Jr.

February, 1966

NO. MTI-66TR7

DATE: February, 1966

TECHNICAL REPORT

ON THE SLOWLY TIME DEPENDENT PROBLEM OF SQUEEZE FILM BEARINGS

by

C.H.T. Pan
T. Chiang
H.G. Elrod, Jr.

Author (s)

E. B. Arwas

Approved

Approved

Prepared for

NATIONAL AERONAUTICS AND SPACE ADMINISTRATION
GEORGE C. MARSHALL SPACE FLIGHT CENTER
HUNTSVILLE, ALABAMA

Prepared under

Contract: NAS 8-11678

MTI
MECHANICAL TECHNOLOGY INCORPORATED

968 ALBANY - SHAKER ROAD — LATHAM, NEW YORK — PHONE 785-0922

ABSTRACT

24995

The stability and vibration response of a spherical squeeze-film hybrid bearing were analyzed theoretically. Since the squeeze frequency is typically much higher than the vibration frequency, the asymptotic analysis for large squeeze number can be applied here. Perturbation solutions about the radially concentric position were obtained for small vibration amplitudes and small radial displacement. There is no limitation, however, in the values of vibration number, (so long as it is small in comparison with the squeeze number), compressibility number, axial displacement ratio and excursion ratio. Dynamic bearing reactions were computed based on the perturbation solutions. Results indicate that a spherical squeeze-film bearing is always stable in the axial direction. In the radial direction, however, instability about the radially concentric position is possible when there is journal rotation; the frequency of instability is exactly one half the rotational frequency; the system would be stable if the mass is kept below the critical value.

The analysis can be readily extended to compute the response to vibratory excitation in either the axial or the radial direction.

Author

TABLE OF CONTENTS

INTRODUCTION

As in all other suspension systems, the dynamic characteristics of a squeeze-film bearing must be considered in order to determine its response to dynamic excitations such as shock load, random excitation, and stability. In squeeze-film bearings the problem is peculiar because the squeeze motion provides a built-in time-dependence in spite of any additional time dependence related to the dynamic excitations. Fortunately, under typical circumstances of interest, the duration of squeeze motion is at least one order of magnitude smaller than the time scale of the dynamic excitation. For example,the squeeze motion may be at 25 kHz where as the duration of a shock load may be about 0.001 sec. The situation is similar to a frequency modulated signal with the squeeze motion being analogous to the high frequency carrier. Elrod postulated that the two time scales are separable.(His derivation is given in Appendix B.) Thus the motion due to dynamic excitation can be treated as quasi-static during each cycle of squeeze motion. Averaging over a cycle of squeeze-motion, he derived the governing equation and established the appropriate boundary conditions for the "slow time dependent problem" assuming that the frequency of squeeze-motion is infinitely high. This equation places no restriction on either the amplitudes or the type of time dependence. However, a large class of dynamic problems of practical interest is related to simple, harmonic motions of small amplitudes; for instance, one is generally interested in the frequency response for the range 20 Hz - 2 kHz, from which responses to random and impulse excitations can be constructed with the aid of Fourier transformations, and the onset of self-excited instability can also be determined. For this reason, we give particular attention to the solution of Elrod's equation for small amplitude harmonic motions.

The spherical squeeze-film bearing has become a leading candidate for the suspension of the output of a precision gyroscope. Its advantages include relative ease in manufacturing, freedom from need for critical alignment, and its adaptability to an effective transducer design. Of particular interest is

a pair of spherical bearings having their squeeze motion provided by an axial transducer. As a first approximation, the squeeze motion of the bearing can be regarded to be uniform and purely axial. Elrod's equation will be solved for such a bearing under the condition that a "low frequency" harmonic motion of small amplitude corresponding to a dynamic response of the float is superimposed on the "high frequency" squeeze motion.

2. ANALYSIS

In analyzing the stability and vibration response of a squeeze-film bearing, it is essential to have information about the dynamic bearing reactions from gas film pressure forces due to perturbed periodic motion of the journal.

2.1. Basic Equations

Let us consider the isothermal Reynolds' Equation of a spherical squeeze-film bearing with meridian journal angular speed ω and squeeze frequency Ω (Ref. 1)

$$\sin\phi \frac{\partial}{\partial\phi}\left[\sin\phi\ H^3\ P \frac{\partial P}{\partial\phi}\right] + \frac{\partial}{\partial\theta}\left[H^3\ P \frac{\partial P}{\partial\theta}\right] = \left(\frac{R}{C}\right)^2 \sin^2\phi \left[\frac{6\mu\omega}{p_a}\frac{\partial}{\partial\theta} + \frac{12\mu}{p_a}\frac{\partial}{\partial t}\right]\Psi \quad \ldots\ldots\ldots\ldots \quad (2.1)$$

where $\Psi \equiv PH$. $\ldots\ldots\ldots\ldots\ldots\ldots\ldots\ldots\ldots\ldots$ (2.2)

We have used the spherical coordinates with θ and ϕ the meridianal and azimuthal angles respectively. The bearing extends in the ϕ-direction from ϕ_1 to ϕ_2 (see Fig. 1).

Aside from the squeeze frequency Ω, the bearing may have a radial vibration frequency (or whirl speed) ν_r and an axial vibration frequency ν_z. Both the squeeze motion and vibrations contribute to the time dependence of the problem. Hence, we can write formally:

$$\Psi = \Psi(\phi,\theta,T,\tau) \quad \ldots\ldots\ldots\ldots\ldots\ldots\ldots\ldots \quad (2.3.)$$

where

$$\left.\begin{aligned} T &= \nu t \\ \tau &= \Omega t \\ \nu &= \text{vibration frequency} \\ &\quad (\text{axial or radial}) \end{aligned}\right] \quad \ldots\ldots\ldots\ldots\ldots\ldots \quad (2.4.)$$

Thus

$$\frac{\partial\Psi}{\partial t} = \frac{\partial\Psi}{\partial T}\frac{dT}{dt} + \frac{\partial\Psi}{\partial\tau}\frac{d\tau}{dt} \quad \ldots\ldots\ldots\ldots\ldots\ldots\ldots\ldots \quad (2.5)$$

Substituting (2.5) into Equation (2.1) we obtain:

$$\sin\phi\,\frac{\partial}{\partial\phi}\left[\sin\phi\;\; H^3P\,\frac{\partial P}{\partial\phi}\right] + \frac{\partial}{\partial\theta}\left[H^3P\,\frac{\partial P}{\partial\theta}\right]$$
$$= \sin^2\phi\left[\Lambda\,\frac{\partial}{\partial\theta} + \zeta\,\frac{\partial}{\partial T} + \sigma\,\frac{\partial}{\partial\tau}\right]\Psi \qquad \ldots\ldots\ldots\ldots\ldots\ldots \quad (2.6)$$

where

$$\left.\begin{aligned}\Lambda &= \text{compressibility number} = \frac{6\mu\omega}{p_a}\left(\frac{R}{C}\right)^2\\ \zeta &= \text{vibration number} = \frac{12\mu\nu}{p_a}\left(\frac{R}{C}\right)^2\\ \sigma &= \text{squeeze number} = \frac{12\mu\Omega}{p_a}\left(\frac{R}{C}\right)^2\end{aligned}\right] \qquad \ldots\ldots\ldots\ldots\ldots\ldots \quad (2.7)$$

In this manner, we have introduced separate time scales for journal vibration (as a rigid body) and bearing squeeze motion.

We shall further assume that the squeeze motion is entirely in the axial direction, although the general approach is equally applicable to any other squeeze motion. We shall normalize all displacements with respect to the nominal bearing clearance, C. Setting ε = excursion ratio, η_z, η_r = axial and radial displacement ratio respectively, δ_z = axial vibration amplitude ratio, δ_x,δ_y = components of radial vibration amplitude ratio, where x denotes the direction of η_r and y, perpendicular to it (see Fig. 2); the normalized film gap can be expressed as (Refs. 1 and 4)

$$H = H_\infty + \varepsilon\cos\phi\cos\tau \qquad \ldots\ldots\ldots\ldots\ldots\ldots \quad (2.8)$$

where

$$H_\infty = 1 + \eta_z\cos\phi + \eta_r\sin\phi\cos\theta + \delta_z\cos\phi\cos\nu_z(t - t_z) + (\delta_x\cos\theta + \delta_y\sin\theta)\sin\phi\cos\nu_r(t-t_r) \quad (2.9)$$

t_z d t_r are reference times for the two respective motions.

The boundary conditions of Eq. (2.1) are

$$P(\phi_1,\theta, T,\tau) = 1 \qquad \ldots\ldots\ldots\ldots\ldots\ldots \quad (2.10)$$
$$P(\phi_2,\theta, T,\tau) = 1 \qquad \ldots\ldots\ldots\ldots\ldots\ldots \quad (2.11)$$
$$P(\phi,\theta, T,\tau) = P(\phi, \theta+2\pi, T,\tau) \qquad \ldots\ldots\ldots\ldots\ldots\ldots \quad (2.12)$$
$$\frac{\partial P(\phi,\theta, T,\tau)}{\partial\theta} = \frac{\partial P(\phi, \theta+2\pi, T,\tau)}{\partial\theta} \qquad \ldots\ldots\ldots\ldots\ldots\ldots \quad (2.13)$$

where T is either $\nu_z(t-t_z)$ or $\nu_r(t-t_r)$, since the problems of the respective motions are separable as will be shown later. Since the squeeze frequency is typically much higher than both the vibration frequency and the journal rotating speed, it is of interest to study the asymptotic behavior of the solution as $\sigma\to\infty$ with Λ and ζ held fixed. We also have the relationship between the two time scales,

$$\frac{T}{\tau} = \frac{\nu}{\Omega} << 1 \quad \ldots\ldots\ldots\ldots\ldots\ldots\ldots\ldots \quad (2.14)$$

From Equation (2.14) it is obvious that when the squeeze motion completes a cycle ($\tau = \tau_o \rightarrow \tau_o + 2\pi$), the vibration time T changes only by an amount of $2\pi \frac{\nu}{\Omega}$ which approaches zero as $\Omega \rightarrow \infty$. Therefore, with respect to the high frequency squeeze motion, all vibrations are quasi-stationary. A general treatment of this topic is given in Appendix B. Applying the results of Appendix B to spherical squeeze-film bearings we have

$$\text{as } \sigma \rightarrow \infty, \quad \Psi = \Psi_\infty \ (\phi, \theta, T) \quad \ldots\ldots\ldots\ldots\ldots\ldots \quad (2.15)$$

where Ψ_∞ is the asymptotic solution of Ψ for large σ in the interior of the bearing film, i.e. the whole bearing film excluding the narrow regions near the edges ($\phi = \phi_1$ and $\phi = \phi_2$). These narrow regions are called the boundary layers, the extent of which is of the order of $1/\sqrt{\sigma}$.

The governing equation for Ψ_∞ is

$$\sin\phi \frac{\partial}{\partial\phi} \left[\sin\phi \frac{\partial}{\partial\phi} (H_\infty \Psi_\infty^2) - 3\Psi_\infty^2 \sin\phi \frac{\partial H_\infty}{\partial\phi} \right]$$
$$+ \frac{\partial}{\partial\theta} \left[\frac{\partial}{\partial\theta} (H_\infty \Psi_\infty^2) - 3\Psi_\infty^2 \frac{\partial H_\infty}{\partial\theta} \right]$$
$$= \sin^2\phi \left[2\Lambda \frac{\partial \Psi_\infty}{\partial\theta} + \frac{24\mu\nu}{p_a} \left(\frac{R}{C}\right)^2 \frac{\partial \Psi_\infty}{\partial T} \right] \quad \ldots\ldots\ldots\ldots\ldots\ldots \quad (2.16)$$

with boundary conditions

$$(H_\infty \Psi_\infty^2)\Big|_{\phi_i,\theta,T} = H_\infty^3 \ (\phi_i,\theta,T) + \frac{3}{2} \varepsilon^2 \cos^2\phi_i \ H_\infty(\phi_i,\theta,T) \ (i=1,2) \quad \ldots \quad (2.17)$$

Note that we have used the identity

$$H^3 P dP = \frac{1}{2} d\ (H\Psi^2) - \frac{3}{2} \Psi^2 dH \quad \ldots\ldots\ldots\ldots\ldots\ldots \quad (2.18)$$

2.2. Perturbation Solutions - small η_r, δ_z, δ_x and δ_y

The asymptotic solution Ψ_∞ governed by Eq. (2.16) and subject to boundary conditions (2.17) plus the periodicity conditions in θ, will be solved in this section. For small η_r, δ_z, δ_x and δ_y the problem may be solved by perturbation method.

Following the ideas of Reference 5, we use the identities

$$\left.\begin{aligned} \cos\theta \cos T_r &= \frac{1}{2}\left[\cos(\theta - T_r) + \cos(\theta + T_r)\right] \\ \sin\theta \cos T_r &= \frac{1}{2}\left[\sin(\theta - T_r) + \sin(\theta + T_r)\right] \end{aligned}\right\} \quad \ldots\ldots\ldots \quad (2.19)$$

Then Equation (2.9) becomes

$$\begin{aligned} H_\infty = {} & 1 + \eta_z \cos\phi + \eta_r \sin\phi \cos\theta \\ & + \sin\phi \left[\frac{1}{2}\delta_x \cos(\theta - T_r) + \frac{1}{2}\delta_x \cos(\theta + T_r) \right. \\ & \qquad \left. + \frac{1}{2}\delta_y \sin(\theta - T_r) + \frac{1}{2}\delta_y \sin(\theta + T_r)\right] \\ & + \delta_z \cos\phi \cos T_z \end{aligned} \quad \ldots\ldots\ldots\ldots\ldots\ldots \quad (2.20)$$

where

$$\left.\begin{aligned} T_r &= \nu_r (t - t_r) \\ T_z &= \nu_z (t - t_z) \end{aligned}\right] \quad \ldots\ldots\ldots\ldots\ldots\ldots \quad (2.20a)$$

For small perturbations it is convenient to expand

$$\begin{aligned} H_\infty \Psi_\infty^2 = {} & g_o + \eta_r \, \mathrm{Re}\left\{e^{i\theta} g_1\right\} \\ & + \frac{\delta_x}{2} \mathrm{Re}\left\{e^{i(\theta - T_r)} g_2 + e^{i(\theta + T_r)} g_3\right\} \\ & + \frac{\delta_y}{2} \mathrm{Re}\left\{-i e^{i(\theta - T_r)} g_4 - i e^{i(\theta - T_r)} g_5\right\} \\ & + \delta_z \, \mathrm{Re}\{e^{i T_z} g_z\} \end{aligned} \quad \ldots\ldots\ldots\ldots\ldots\ldots \quad (2.21)$$

Rewrite Eq. (2.20) in the form

$$\begin{aligned} H_\infty = {} & h_o + \eta_r \, \mathrm{Re}\left\{h_1 e^{i\theta}\right\} \\ & + \frac{\delta_x}{2} \mathrm{Re}\left\{h_1 e^{i(\theta - T_r)} + h_1 e^{i(\theta + T_r)}\right\} \\ & + \frac{\delta_y}{2} \mathrm{Re}\left\{-i h_1 e^{i(\theta - T_r)} - i h_1 e^{i(\theta - T_r)}\right\} \\ & + \delta_z \, \mathrm{Re}\{\cos\phi \, e^{i T_z}\} \end{aligned} \quad \ldots\ldots\ldots\ldots\ldots\ldots \quad (2.22)$$

where

$$\left.\begin{aligned} h_o &= 1 + \eta_z \cos\phi \\ h_1 &= \sin\phi \end{aligned}\right] \quad \ldots\ldots\ldots\ldots\ldots\ldots\ldots \quad (2.23)$$

Substituting (2.21) into Equation (2.16) and noting that

$$\frac{\nu}{\omega}\frac{\partial}{\partial T} = \frac{1}{\omega}\frac{\partial}{\partial t} \quad \ldots\ldots\ldots\ldots\ldots\ldots\ldots \quad (2.24)$$

we obtain

$$\sin\phi \frac{d}{d\phi}\left[\sin\phi\left(\frac{dg_o}{d\phi} - 3\frac{g_o}{h_o}\frac{dh_o}{d\phi}\right)\right] = 0 \quad \ldots\ldots\ldots\ldots \quad (2.25)$$

$$\sin\phi \frac{d}{d\phi}\left\{\sin\phi\left[\frac{dg_j}{d\phi} - 3\frac{g_j}{h_o}\frac{dh_o}{d\phi} - 3g_o\frac{d}{d\phi}\left(\frac{h_1}{h_o}\right)\right]\right\} - g_j + 3g_o\frac{h_1}{h}$$

$$- i\Lambda_j \sin^2\phi\sqrt{\frac{g_o}{h_o}}\left(\frac{g_j}{g_o} - \frac{h_1}{h_o}\right) = 0 \qquad (j = 1,2,3,4,5) \ldots\ldots\ldots \quad (2.26)$$

and

$$\sin\phi \frac{d}{d\phi}\left\{\sin\phi\left[\frac{dg_z}{d\phi} - 3\frac{g_z}{h_o}\frac{dh_o}{d\phi} - 3g_o\frac{d}{d\phi}\left(\frac{\cos\phi}{h_o}\right)\right]\right\}$$

$$- i\zeta_z \sin^2\phi\sqrt{\frac{g_o}{h_o}}\left(\frac{g_z}{g_o} - \frac{\cos\phi}{h_o}\right) = 0 \quad \ldots\ldots\ldots\ldots\ldots \quad (2.27)$$

where

$$\left.\begin{aligned} \Lambda_1 &= \Lambda \\ \Lambda_2 &= \Lambda_4 = \Lambda\left(1 - 2\frac{\nu_r}{\omega}\right) \\ \Lambda_3 &= \Lambda_5 = \Lambda\left(1 + 2\frac{\nu_r}{\omega}\right) \\ \zeta_z &= \frac{12\mu\nu_z}{p_a}\left(\frac{R}{C}\right)^2 = \text{axial vibration number} \end{aligned}\right] \quad \ldots\ldots\ldots \quad (2.28)$$

The boundary conditions are, from Equation (2.17),

$$g_o(\phi_i) = h_o^3(\phi_i) + \frac{3}{2} h_o(\phi_i)\,\varepsilon^2\cos^2\phi_i \qquad (i = 1,2) \ldots\ldots \quad (2.29)$$

$$g_j(\phi_i) = 3h_o^2(\phi_i)\,h_1(\phi_i) + \frac{3}{2} h_1(\phi_i)\,\varepsilon^2\cos^2\phi_i \qquad (i = 1,2)\ (j = 1,2,3,4,5) \quad (2.30)$$

$$g_z(\phi_i) = 3h_o^2(\phi_i)\cos\phi_i + \frac{3}{2}\varepsilon^2\cos^3\phi_i \qquad (i = 1,2) \quad (2.31)$$

Thus, it is seen that the linearized perturbation solutions are not coupled and the method of superposition can be applied. Any small vibrations in a direction perpendicular to the z-axis, for instance, the δ_x-term in Eq. (2.22) , may be considered as the combination of the "forward" and "backward" whirls. The corresponding solutions are obviously g_2 and g_3 (see Eq.(2.21)).

The solution g_o satisfying Equations (2.25) and (2.29) has been obtained in Ref. 4. This represents the solution of an axially displaced, but radially concentric spherical squeeze-film bearing. The solution g_1 was also obtained in Reference 4. The function g_j (j = 2,3,4,5), (satisfying Eqs. (2.26) and (2.30)), differ from g_1 only in the numerical value for Λ_j. Therefore, knowing g_1 we can obtain g_j (j = 2,3,4,5) immediately using the proper numerical value for Λ_j. Since $\Lambda_2 = \Lambda_4$ and $\Lambda_3 = \Lambda_5$, we have

$$\left.\begin{aligned} g_2 &= g_4 \\ \text{and } g_3 &= g_5 \end{aligned}\right] \qquad \ldots\ldots\ldots\ldots\ldots\ldots\ldots\ldots \qquad (2.32)$$

Separating the real and imaginary parts,

$$\left.\begin{aligned} g_1 &= u_1 + i\, v_1 \\ g_2 &= u_2 + i\, v_2 \\ g_3 &= u_3 + i\, v_3 \end{aligned}\right] \qquad \ldots\ldots\ldots\ldots\ldots\ldots\ldots\ldots \qquad (2.33)$$

The u's and v's may be regarded as known functions using the solutions of Ref. 4 with proper values of Λ's.

Note that Λ_j may take on negative values for any ν_r greater than $\omega/2$. Then Eq. (2.26)together with boundary conditions (2.30) suggests that

$$\left.\begin{aligned} u_j\,(-\Lambda_j) &= u_j\,(\Lambda_j) \\ v_j\,(-\Lambda_j) &= -v_j\,(\Lambda_j) \end{aligned}\right] \qquad \ldots\ldots\ldots\ldots\ldots\ldots\ldots\ldots \qquad (2.34)$$

The above relationships will be used later.

Since g_z may be complex, we separate its real and imaginary parts,

$$g_z = u_z + v_z \qquad \ldots\ldots\ldots\ldots\ldots\ldots\ldots\ldots \qquad (2.35)$$

Then Equations (2.27) and (2.31) yield

$$\frac{d^2u_z}{d\phi^2} + f_1(\phi)\frac{du_z}{d\phi} + f_2(\phi)\,u_z + \zeta_z\sqrt{\frac{g_o}{h_o}}\,\frac{1}{g_o}\,v_z = 3\frac{d\,f_3(\phi)}{d\phi} + 3(\cot\phi)\,f_3(\phi) \quad \ldots\ldots\ldots\ldots \quad (2.36a)$$

$$\frac{d^2v_z}{d\phi^2} + f_1(\phi)\frac{dv_z}{d\phi} + f_2(\phi)\,v_z - \zeta_z\sqrt{\frac{g_o}{h_o}}\,\frac{1}{g_o}\,u_z = -\zeta_z\sqrt{\frac{g_o}{h_o}}\,\frac{\cos\phi}{h_o} \quad \ldots\ldots\ldots\ldots\ldots\ldots \quad (2.36b)$$

with boundary conditions,

$$u_z(\phi_i) = 3\,h_o^2(\phi_i)\cos\phi_i + \frac{3}{2}\,\varepsilon^2\cos^3\phi_i \qquad (i = 1,2) \ldots\ldots \quad (2.37)$$

$$v_z(\phi_i) = 0 \qquad (i = 1,2) \ldots\ldots \quad (2.38)$$

where

$$\left.\begin{aligned} f_1(\phi) &= -\frac{3}{h_o}\frac{dh_o}{d\phi} + \cot\phi \\ f_2(\phi) &= -3\frac{d}{d\phi}\left(\frac{1}{h_o}\frac{dh_o}{d\phi}\right) - 3(\cot\phi)\frac{1}{h_o}\frac{dh_o}{d\phi} \\ f_3(\phi) &= -\frac{g_o}{h_o}\sin\phi - \frac{g_o\cos\phi}{h_o^2}\frac{dh_o}{d\phi} \end{aligned}\right\} \quad \ldots\ldots \quad (2.39)$$

Equations (2.36a) and (2.36b) with boundary conditions (2.37) and (2.38) are to be solved numerically using the matrix multiplication method described in Appendix A.

3. DYNAMIC BEARING REACTIONS

Using the results of the asymptotic analysis and the perturbation solutions of the previous section, we can calculate the dynamic bearing reactions.

The pressure distribution of large σ is related to the asymptotic solution Ψ_∞ by

$$P = \frac{1}{H}\sqrt{\frac{H_\infty \Psi_\infty^2}{H_\infty}} = \frac{1}{H_\infty + \varepsilon\cos\phi\ \cos\tau}\sqrt{\frac{H_\infty \Psi_\infty^2}{H_\infty}} \quad \ldots\ldots\ldots\ldots \quad (3.1)$$

which may be readily expanded into

$$\begin{aligned} P = \frac{1}{h_o + \varepsilon\cos\phi\ \cos\tau}\sqrt{\frac{g_o}{h_o}}\ \mathrm{Re}\ \Bigg\{ & 1 + \eta_r\, e^{i\theta}\left[\frac{g_1}{2g_o} - \frac{h_1}{2h_o} - \frac{h_1}{h_o + \varepsilon\cos\phi\ \cos\tau}\right] \\ & + \left(\frac{\delta_x}{2} - i\,\frac{\delta_y}{2}\right) e^{i(\theta - T_r)}\left[\frac{g_2}{2g_o} - \frac{h_1}{2h_o} - \frac{h_1}{h_o + \varepsilon\cos\phi\ \cos\tau}\right] \\ & + \left(\frac{\delta_x}{2} - i\,\frac{\delta_y}{2}\right) e^{i(\theta + T_r)}\left[\frac{g_3}{2g_o} - \frac{h_1}{2h_o} - \frac{h_1}{h_o + \varepsilon\cos\phi\ \cos\tau}\right] \\ & + \delta_z\, e^{iT_z}\left[\frac{g_z}{2g_o} - \frac{\cos\phi}{2h_o} - \frac{\cos\phi}{h_o + \varepsilon\cos\phi\ \cos\tau}\right]\Bigg\} \quad \ldots\ldots\ldots \quad (3.2) \end{aligned}$$

Equation (3.2) contains, first of all, the zeroth-order solution which represents the axially displaced but radially concentric problem plus the contributions from all the perturbations. Among the perturbation terms, the η_r-term represents perturbation due to a steady-state radial displacement; the δ_x and δ_y terms represent perturbation due to radial vibrations; and, finally, the δ_z terms represent perturbation due to an axial vibration. All perturbations are about the radially concentric position. It is to be noted that for small perturbations the axial and radial vibrations are not coupled, i.e. one is not affected by the other.

3.1. Axial Dynamic Reactions

Denoting the δ_z terms of (3.2) by $P_{\delta z}$ we can compute the axial dynamic bearing force

$$F_z = \int_0^{2\pi} \frac{d\tau}{2\pi} \int_{\phi_1}^{\phi_2} p_a P_{\delta_z} \cos\phi \, (2\pi R \sin\phi) \, R \, d\phi \quad \ldots\ldots\ldots\ldots \quad (3.3)$$

or

$$\frac{F_z}{p_a \pi R^2} = \int_0^{2\pi} \frac{d\tau}{2\pi} \int_{\phi_1}^{\phi_2} P_{\delta_z} \, 2 \sin\phi \cos\phi \, d\phi \quad \ldots\ldots\ldots\ldots \quad (3.4)$$

where

$$P_{\delta_z} = \frac{1}{h_o + \varepsilon\cos\phi \cos\tau} \sqrt{\frac{g_o}{h_o}} \, \mathrm{Re} \left\{ \delta_z \, e^{iT_z} \left[\frac{g_z}{2g_o} - \frac{\cos\phi}{2h_o} - \frac{\cos\phi}{h_o + \varepsilon\cos\phi \cos\tau} \right] \right\} \quad \ldots\ldots\ldots \quad (3.5)$$

Now we integrate (3.4) with respect to τ, holding T_z = constant. In so doing, we have used the condition that the axial vibration is quasi-stationary in comparison to the high frequency squeeze motion. This point has been elaborated in App. B and was also mentioned in Section 2. The result of the τ-integration is:

$$\frac{F_z}{p_a \pi R^2} = \delta_z \int_{\phi_1}^{\phi_2} \frac{2\sin\phi \cos\phi}{\sqrt{h_o^2 - \varepsilon^2 \cos^2\phi}} \sqrt{\frac{g_o}{h_o}} \, e^{i T_z} \left[\frac{u_z + i \, v_z}{2 \, g_o} - \frac{\cos\phi}{2h_o} - \frac{h_o \cos\phi}{h_o^2 - \varepsilon^2 \cos^2\phi} \right] d\phi \quad \ldots \quad (3.6)$$

Equations (309) and (317) of Referecen 6 were used above; they are

$$\int_0^{2\pi} \frac{d\tau}{a + b\cos\tau} = \frac{2\pi}{\sqrt{a^2 - b^2}} \quad \ldots\ldots\ldots\ldots\ldots\ldots \quad (3.7)$$

and

$$\int_0^{2\pi} \frac{d\tau}{(a + b\cos\tau)^2} = \frac{2\pi a}{(a^2 - b^2)^{3/2}} \quad \ldots\ldots\ldots\ldots\ldots \quad (3.8)$$

Rewrite Eq. (3.6) in the form

$$\frac{F_z}{p_a \pi R^2} = (-\delta_z)\ \mathrm{Re}\left\{ e^{i\,T_z}\,(U_z + i\,V_z) \right\} \qquad \ldots\ldots\ldots\ldots \quad (3.9)$$

where

$$\left.\begin{aligned} U_z &= \int_{\phi_1}^{\phi_2} \frac{2\sin\phi\cos\phi}{\sqrt{h_o^2-\varepsilon^2\cos^2\phi}} \sqrt{\frac{g_o}{h_o}} \left[\frac{-u_z}{2g_o} + \frac{\cos\phi}{2h_o} + \frac{h_o\cos\phi}{h_o^2-\varepsilon^2\cos\phi} \right] d\phi \\ V_z &= \int_{\phi_1}^{\phi_2} \frac{2\sin\phi\cos\phi}{\sqrt{h_o^2-\varepsilon^2\cos\phi}} \sqrt{\frac{g_o}{h_o}} \left[\frac{-v_z}{2g_o} \right] d\phi \end{aligned}\right\} \ldots \quad (3.10)$$

Note that in Eq. (3.9) we have factored out $(-\delta_z)$. This is because δ_z is positive in the direction of increasing gap whereas the bearing stiffness is defined as "the increment of bearing force per unit decrement of the gap". Clearly, U_z the in-phase component, is the effective dynamic stiffness; and V_z, the out-of-phase component, is the effective dynamic damping. From the numerical solutions of u_z and v_z of the Appendix, U_z and V_z can be integrated numerically. The results are plotted against ζ_z in Figure 3 and 4 for bearing extending from $\phi_1 = 41.5^o$ to $\phi_2 = 68^o$. This geometry is chosen because its steady-state results were already given in Ref. 4.

3.2. Radial Dynamic Reactions

The dynamic bearing forces in a plane perpendicular to the z-axis can be decomposed into x and y components denoted by F_x and F_y (see Fig. 2). Note that $F_x \equiv -F_R$ and $F_y \equiv F_T$. Let

$$P_{\delta_x,\delta_y} = \frac{1}{h_o+\varepsilon\cos\phi\cos\tau} \sqrt{\frac{g_o}{h_o}}\ \mathrm{Re}\left\{ \left(\frac{\delta_x}{2} - i\,\frac{\delta_y}{2} \right) e^{i(\theta-T_r)} \left[\frac{g_2}{2g_o} - \frac{h_1}{2h_o} - \frac{h_1}{h_o+\varepsilon\cos\phi\cos\phi} \right] \right.$$

$$\left. + \left(\frac{\delta_x}{2} - i\,\frac{\delta_y}{2} \right) e^{i(\theta+T_r)} \left[\frac{g_3}{2g_o} - \frac{h_1}{2h_o} - \frac{h_1}{h_o+\varepsilon\cos\phi\cos\tau} \right] \right\} \qquad \ldots\ldots\ldots \quad (3.11)$$

The dynamic bearing forces are obtained by first averaging over a squeeze cycle and then integrating throughout the bearing film,

$$\frac{F_x}{p_a \pi R^2} = \frac{1}{\pi} \int_0^{2\pi} \frac{d\tau}{2\pi} \int_0^{2\pi} \cos\theta \, d\theta \int_{\phi_1}^{\phi_2} P_{\delta_x, \delta_y} \sin^2\phi \, d\phi \quad \ldots\ldots\ldots (3.12)$$

$$\frac{F_y}{p_a \pi R^2} = \frac{1}{\pi} \int_0^{2\pi} \frac{d\tau}{2\pi} \int_0^{2\pi} \sin\theta \, d\theta \int_{\phi_1}^{\phi_2} P_{\delta_x, \delta_y} \sin^2\phi \, d\phi \quad \ldots\ldots\ldots (3.13)$$

Carrying out the integrations and noting that the results are quite analogous to the radial and tangential stiffness of Reference 4, we obtain

$$\frac{F_x}{p_a \pi R^2} = -\cos T_r \left[\frac{\delta_x}{2} \left(K_R^{(2)} + K_R^{(3)} \right) + \frac{\delta_y}{2} \left(K_T^{(2)} + K_T^{(3)} \right) \right] + \sin T_r \left[-\frac{\delta_x}{2} \left(K_T^{(2)} - K_T^{(3)} \right) + \frac{\delta_y}{2} \left(K_R^{(2)} - K_R^{(3)} \right) \right] \quad \ldots (3.14)$$

and

$$\frac{F_y}{p_a \pi R} = \cos T_r \left[\frac{\delta_x}{2} \left(K_T^{(2)} + K_T^{(3)} \right) - \frac{\delta_y}{2} \left(K_R^{(2)} + K_R^{(3)} \right) \right] - \sin T_r \left[\frac{\delta_x}{2} \left(K_R^{(2)} - K_R^{(3)} \right) + \frac{\delta_y}{2} \left(K_T^{(2)} - K_T^{(3)} \right) \right] \quad \ldots (3.15)$$

where

$$K_R^{(j)} = -\int_{\phi_1}^{\phi_2} \frac{\sin^2\phi}{\sqrt{h_o^2 - \varepsilon^2 \cos^2\phi}} \sqrt{\frac{g_o}{h_o}} \left[\frac{u_j}{2g_o} \frac{h_1}{2h_o} - \frac{h_o h_1}{h_o^2 - \varepsilon^2 \cos^2\phi} \, d\phi \right] (i=2,3) \quad (3.16)$$

$$K_T^{(j)} = -\int_{\phi_1}^{\phi_2} \frac{\sin^2\phi}{\sqrt{h_o^2 - \varepsilon^2 \cos^2\phi}} \sqrt{\frac{g_o}{h_o}} \left[\frac{v_j}{2g_o} \right] d\phi \qquad (j=2,3) \ldots \quad (3.17)$$

Note that $K_R^{(j)}$ and $K_T^{(j)}$ are identical to those of Eqs. (4.17) and (4.18) of Reference 4 upon replacing u by u_j and v by v_j (i.e. Λ by Λ_j). The results of Reference 4 for the particular geometry of $\phi_1 = 41.5^\circ$ and $\phi_2 = 68^\circ$ are reproduced here in Figures 5 and 6. The curves for $\eta_z = 0$ and -0.4 are replotted in Figures 7 and 8. The data for negative values of Λ_j in Figs. 7 and 8 can be obtained with the aid of Eq. (2.34). It is seen from Equations (2.34), (3.16) and (3.17) that $K_R^{(j)}$ is an even function of Λ_j whereas $K_T^{(j)}$ is an odd function of Λ_j.

Equations (3.14) and (3.15) can be written in matrix notation

$$\begin{bmatrix} \dfrac{F_x}{p\ \pi R^2} \\ \\ \dfrac{F_y}{p_a \pi R^2} \end{bmatrix} = \begin{bmatrix} Z_{xx} & Z_{xy} \\ \\ Z_{yx} & Z_{yy} \end{bmatrix} \begin{bmatrix} \delta_x \\ \\ \delta_y \end{bmatrix} e^{iT_r} \quad \ldots\ldots\ldots \quad (3.18)$$

taking, of course, only the real part. Note that δ_x and δ_y do not have to be both real.

Here we have denoted

$$\left.\begin{aligned} Z_{xx} &\equiv U_{xx} + i\,V_{xx} \equiv -\frac{1}{2}\left(K_R^{(2)} + K_R^{(3)}\right) + i\,\frac{1}{2}\left(K_T^{(2)} - K_T^{(3)}\right) \\ Z_{xy} &\equiv U_{xy} + i\,V_{xy} \equiv -\frac{1}{2}\left(K_T^{(2)} + K_T^{(3)}\right) - i\,\frac{1}{2}\left(K_R^{(2)} - K_R^{(3)}\right) \\ Z_{yx} &\equiv U_{yx} + i\,V_{yx} \equiv \frac{1}{2}\left(K_T^{(2)} + K_T^{(3)}\right) + i\,\frac{1}{2}\left(K_R^{(2)} - K_R^{(3)}\right) \\ Z_{yy} &\equiv U_{yy} + i\,V_{yy} \equiv -\frac{1}{2}\left(K_R^{(2)} + K_R^{(3)}\right) + i\,\frac{1}{2}\left(K_T^{(2)} - K_T^{(3)}\right) \end{aligned}\right\} \quad \ldots \quad (3.19)$$

Note that $Z_{xx} = Z_{yy}$ and $Z_{xy} = -Z_{yx}$; which indicate that the bearing is isotropic according to the definition of Ref. 3. This result should have been obvious since the bearing geometry possesses rotational symmetry and that a concentric equilibrium position was used in the dynamic perturbation analysis.

4. STABILITY OF AXIAL VIBRATIONS

In the previous sections we have shown that for small perturbations the axial vibration and radial vibration are not coupled. Therefore, we can deal with the axial and radial stability problems separately. The axial stability is thus reduced to a single degree-of-freedom problem.

The results of stability analysis of Reference 3 for a single degree-of-freedom system may be stated as follows:

Let ν_{zo} be the frequency of axial vibration at which

$$V_z\Big|_{\nu_{zo}} = 0 \quad \ldots\ldots\ldots\ldots\ldots\ldots\ldots\ldots \quad (4.1)$$

This is the state of neutral stability. Then, the critical mass is given by

$$M_o = \frac{p_a \pi R^2}{C \nu_{zo}^2} U_z\Big|_{\nu_{zo}} \quad \ldots\ldots\ldots\ldots\ldots\ldots \quad (4.2)$$

A slight variation from the state of neutral stability would cause the system to be unstable if and only if

$$\frac{\partial V_z}{\partial \nu_z}\Big|_{\nu_{zo}} \delta M > 0 \quad \ldots\ldots\ldots\ldots\ldots\ldots\ldots\ldots \quad (4.3)$$

where δM is a small mass increment above M_o.

Using the above results of Reference 3, and from Figure 4, it is seen that V_z is zero only when $\zeta_z = 0$ or $\nu_z = 0$. Hence we have

$$\nu_{zo} = 0 \quad \ldots\ldots\ldots\ldots\ldots\ldots\ldots\ldots \quad (4.4)$$

Since U_z does not vanish at ν_{zo}, Eq. (4.2) yields

$$M_o = \infty \quad \ldots\ldots\ldots\ldots\ldots\ldots\ldots\ldots \quad (4.5)$$

Therefore, any actual mass would be less than the critical mass and

$$\delta M < 0 \quad \ldots\ldots\ldots\ldots\ldots\ldots\ldots\ldots \quad (4.6)$$

Also, we have

$$\left.\frac{\partial V_z}{\partial \nu_z}\right|_{\nu_{zo}} = \left[\frac{\partial V_z}{\partial \zeta_z}\ \frac{d\zeta_z}{d\nu_z}\right]_{\nu_{zo}} > 0 \qquad \ldots\ldots\ldots\ldots\ldots \quad (4.7)$$

Combination of (4.6) and (4.7) results in

$$\left.\frac{\partial V_z}{\partial \nu_z}\right|_{\nu_{zo}} \partial M < 0 \qquad \ldots\ldots\ldots\ldots\ldots\ldots\ldots\ldots \quad (4.8)$$

Thus, we conclude that a spherical squeeze-film bearing is always stable in the axial direction. The same conclusion can be said of the flat squeeze-film thrust bearing, since it may be considered to be the special case of a spherical bearing with small subtended angles (ϕ_1 and ϕ_2).

5. RADIAL STABILITY AND VIBRATION RESPONSE

The radial dynamic bearing forces were obtained in Section 3.2. using perturbation solutions about the radially concentric position. The results, therefore, represent dynamic reactions of an unloaded (radially) spherical squeeze-film bearing.

5.1. Radial Stability

The stability of an isotropic bearing of two degrees of freedom was analyzed in Reference 3. Since the axial vibration and radial vibration of a spherical squeeze-film bearing are decoupled for small perturbations, the radial stability of a radially unloaded spherical squeeze-film bearing may be studied using the isotropic bearing results of Reference 3 which are summarized as follows:

Let ν_{ro} be the frequency at which

$$K_T^{(j)}(\Lambda_j)\Big|_{\nu_{ro}} = 0 \qquad \ldots\ldots\ldots\ldots\ldots\ldots\ldots\ldots \quad (5.1)$$

Then, with the dimensionless mass defined as

$$m \equiv \frac{M\,C\,\omega^2}{p_a\,\pi\,R^2} \qquad \ldots\ldots\ldots\ldots\ldots\ldots\ldots\ldots \quad (5.2)$$

the critical mass is given by

$$m_o = \frac{K_R^{(j)}(\Lambda_j)\Big|_{\nu_{ro}}}{(\nu_{ro}/\omega)^2} \qquad \ldots\ldots\ldots\ldots\ldots\ldots\ldots\ldots \quad (5.3)$$

A slight variation δm from m_o would cause the system to be unstable if and only if

$$\frac{\partial K_T^{(j)}(\Lambda_j)}{\partial \nu_r}\Bigg|_{\nu_{ro}} \delta m < 0 \qquad \ldots\ldots\ldots\ldots\ldots\ldots\ldots\ldots \quad (5.4)$$

Example: Unloaded (radially) spherical squeeze-film hybrid bearing

Given: $\phi_1 = 41.5^o \quad \phi_2 = 68^o$

$\varepsilon = 0.4$

From Fig. 6, $K_T^{(j)} = 0$, when $\Lambda_j = 0$

Then Eq. (2.28) shows that

$$\Lambda_3 = 1 + 2\frac{\nu_r}{\omega} \neq 0$$

and the only possibility is

$$\Lambda_2 = 1 - 2\frac{\nu_r}{\omega} = 0$$

Thus,

$$\nu_{ro} = \frac{1}{2}\ \omega \quad \ldots\ldots\ldots\ldots\ldots\ldots\ldots\ldots\ldots\ldots \quad (5.5)$$

This indicates that the only possibility of instability of the system is in the form of a half-frequency whirl. From Equation (5.3) and Figure 5, the critical mass is

$$\left.\begin{aligned} m_o &= \frac{0.036}{(1/2)^2} = 0.144 \qquad \text{for } \eta_z = 0.2 \\ m_o &= \frac{0.05}{(1/2)^2} = 0.2 \qquad \text{for } \eta_z = 0 \\ m_o &= \frac{0.076}{(1/2)^2} = 0.304 \qquad \text{for } \eta_z = -0.2 \end{aligned}\right\} \quad \ldots\ldots\ldots\ldots \quad (5.6)$$

Note that in Eq. (5.3), because $\Lambda_j = \Lambda_2 = 0$, $K_R^{(j)}(\Lambda_j)\Big|_{\nu_{ro}}$ is essentially the static radial stiffness of a non-rotating journal. It is seen that the critical mass increases with increasing axial load (decreasing η_z).

Now,

$$\frac{\partial K_T^{(j)}(\Lambda_j)}{\partial \nu_r}\bigg|_{\nu_{ro}} = \frac{\partial K_T^{(2)}(\Lambda_2)}{\partial \Lambda_2}\ \frac{d\Lambda_2}{d\nu_r}\bigg|_{\nu_{ro}} < 0 \quad \ldots\ldots\ldots \quad (5.7)$$

since

$$\frac{\partial K_T(2)}{\partial \Lambda_2}\bigg|_{\nu_{ro}} > 0$$

and

$$\left.\frac{d\,\Lambda_2}{d\nu_r}\right|_{\nu_{ro}} = -\frac{2}{\omega} < 0$$

Combining (5.4) and (5.7) it is seen that the system is unstable if and only if $\delta m > 0$. Conversely, in order for the system to be stable, the mass must be kept below the critical mass. Equation (5.6) then indicates that the axial loading of a radially unloaded spherical squeeze-film hybrid bearing helps to stabilize the system.

5.2. Vibration Response

The vibration response of a spherical squeeze-film hybrid bearing in a plane perpendicular to the z-axis may be obtained by using the dynamic bearing reactions of Section 3. Let us rewrite Eq. (3.18)

$$\begin{bmatrix} \dfrac{F_x}{p_a \pi R^2} \\ \dfrac{F_y}{p_a \pi R^2} \end{bmatrix} = \begin{bmatrix} Z_{xx} & Z_{xy} \\ Z_{yx} & Z_{yy} \end{bmatrix} \begin{bmatrix} \delta_x \\ \delta_y \end{bmatrix} e^{iT_r} \qquad \ldots\ldots\ldots\ldots\ldots \quad (5.8)$$

Recall that δ_x and δ_y do not have to be both real, since the x- and y-vibrations may be out-of-phase. Now we may interpret F_x and F_y as the components of a given force exerted on the journal, and write

$$\begin{bmatrix} \dfrac{F_x}{p_a \pi R^2} \\ \dfrac{F_y}{p_a \pi R^2} \end{bmatrix} = \begin{bmatrix} f_x \\ f_y \end{bmatrix} e^{iT_r} \qquad \ldots\ldots\ldots\ldots\ldots\ldots\ldots \quad (5.9)$$

where f_x and f_y are unit complex force amplitude. Then, corresponding to F_x and F_y, the complex amplitude of the journal motion may be found from

$$\begin{bmatrix} \delta_x \\ \delta_y \end{bmatrix} = \begin{bmatrix} Z_{xx} & Z_{xy} \\ Z_{yx} & Z_{yy} \end{bmatrix}^{-1} \begin{bmatrix} f_x \\ f_y \end{bmatrix} \qquad \ldots\ldots\ldots\ldots\ldots \quad (5.10)$$

The inverse of the Z-matrix can be easily computed with Z_{xx}, Z_{xy}, Z_{yx} and Z_{yy} given by (3.19). Knowing δ_x and δ_y, the motion of the journal is readily obtained from $\mathrm{Re}(\delta_x\, e^{iT}r)$ and $\mathrm{Re}\,(\delta_y\, e^{iT}r)$.

6. CONCLUSIONS

On the basis of the analyses in the previous sections, we conclude the following:

a. When a slowly time dependent motion is superimposed on a high frequency squeeze motion, the fluid film pressure can be found by an asymptotic analysis. In the asymptotic analysis the product of pressure and film thickness is only slowly time dependent.

b. Dynamic bearing reactions are obtained based on perturbation solutions due to small periodic motions of the journal about the radially concentric position.

c. Spherical squeeze-film bearings are always stable in the axial direction. The same conclusions can be said of the flat squeeze-film thrust bearing, since it may be considered to be the special case of a spherical bearing with small subtended angles (ϕ_1 and ϕ_2).

d. Radial instability of a radially unloaded bearing occurs only in the form of half-frequency whirl of a rotating journal. The system would be stable if the mass is kept below the critical value. Axial loading of a radially unloaded, spherical, squeeze-film hybrid bearing helps to stabilize the system. Conversely, the non-rotating journal cannot experience instability according to the present analysis.

e. The present analysis can be readily extended to compute the response to vibratory excitation in either the radial or the axial direction.

ACKNOWLEDGEMENT

The authors wish to thank Dr. V. Castelli for bringing to their attention the matrix-multiplication method for solving differential equations, and Mr. J. Michaud for carrying out the programming and numerical computation.

APPENDIX A-THE MATRIX MULTIPLICATION METHOD IN SOLVING ORDINARY DIFFERERENTIAL EQUATIONS WITH "TWO-POINT" BOUNDARY CONDITIONS*

Equations (2.36a) and (2.36b) together with their boundary conditions (2.37) and (2.38) may be written in the following general form:

$$\text{D.E.} \begin{cases} u'' + f_1 u' + f_2 u + f_3 v'' + f_4 v' + f_5 v = f_6 & \ldots\ldots \text{(A-1)} \\ v'' + g_1 v' + g_2 v + g_3 u'' + g_4 u' + g_5 u = g_6 & \ldots\ldots \text{(A-2)} \end{cases}$$

$$\text{B.C.} \begin{cases} \text{at } x = x_1, \quad u = F, \quad v = G & \ldots\ldots\ldots\ldots\ldots\ldots \text{(A-3)} \\ \text{at } x = x_2, \quad u = \overline{F}, \quad v = \overline{G} & \ldots\ldots\ldots\ldots\ldots\ldots \text{(A-4)} \end{cases}$$

Here we denote the independent variable by x. The primes represent derivations with respect to x. The symbols f_1, f_2 . . . etc. are known functions of x.

In central difference form we can write

$$\left.\begin{aligned} u(x_k) &= u^k \\ u'(x_k) &= \frac{u^{k+1} - u^{k-1}}{2\Delta} \\ u''(x_k) &= \frac{u^{k+1} - 2u^k + u^{k-1}}{\Delta^2} \end{aligned}\right\} \quad \ldots\ldots\ldots\ldots\ldots\ldots \text{(A-5)}$$

We have assumed that there are N divisions between x_1 and x_2, so that $k = 0, 1, 2, \ldots N$, and $\Delta = \frac{x_2 - x_1}{N}$.

Now, Eq. (A-1) take the form

$$u^{k+1}\left[\frac{1}{\Delta^2} + \frac{f_1^k}{2\Delta}\right] + u^k\left[\frac{-2}{\Delta^2} + f_2^k\right] + u^{k-1}\left[\frac{1}{\Delta^2} - \frac{f_1^k}{2\Delta}\right]$$
$$+ v^{k+1}\left[\frac{f_3^k}{\Delta^2} + \frac{f_4^k}{2\Delta}\right] + v^k\left[\frac{-2f_3^k}{\Delta^2} + f_5^k\right] + v^{k-1}\left[\frac{f_3^k}{\Delta^2} - \frac{f_4^k}{2\Delta}\right] = f_6^k \quad \ldots \text{(A-6)}$$

A similar equation may be obtained from Eq. (A-2), which together with (A-6) can be written in the following matrix form,

$$A^k y^{k+1} + B^k y^k + C^k y^{k-1} = d^k \quad \ldots\ldots\ldots\ldots\ldots\ldots \text{(A-7)}$$

---

*The method of computation described in this Appendix is due to Castelli and Pirvics (Ref. 7).

where

$$y^{(\,)} = \begin{bmatrix} u^{(\,)} \\ v^{(\,)} \end{bmatrix}$$

$$A^k = \begin{bmatrix} \frac{1}{\Delta^2} + \frac{f_1^k}{2\Delta} & \frac{f_3^k}{\Delta^2} + \frac{f_4^k}{2\Delta} \\ \frac{g_3^k}{\Delta^2} + \frac{g_4^k}{2\Delta} & \frac{1}{\Delta^2} + \frac{g_1^k}{2\Delta} \end{bmatrix}$$

$$B^k = \begin{bmatrix} \frac{-2}{\Delta^2} + f_2^k & \frac{-2f_3^k}{\Delta^2} + f_5^k \\ \frac{-2g_3^k}{\Delta^2} + g_5^k & \frac{-2}{\Delta^2} + g_2^k \end{bmatrix} \qquad \text{. . . . . (A-8)}$$

$$C^k = \begin{bmatrix} \frac{1}{\Delta^2} - \frac{f_1^k}{2\Delta} & \frac{f_3^k}{\Delta^2} - \frac{f_4^k}{2\Delta} \\ \frac{g_3^k}{\Delta^2} - \frac{g_4^k}{2\Delta} & \frac{1}{\Delta^2} - \frac{g_1^k}{2\Delta} \end{bmatrix}$$

$$d^k = \begin{bmatrix} f_6^k \\ g_6^k \end{bmatrix}$$

Assume that the y-vector at station "k + 1" can be expressed by

$$y^{k+1} = M^k y^k + m^k \qquad \text{. . . . . (A-9)}$$

where M is an unknown matrix and m, an unknown vector. From (A-9) we can write formally

$$\left.\begin{aligned} y^k &= M^{k-1}\, y^{k-1} + m^{k-1} \\ \text{and} \\ y^{k-1} &= M^{k-2}\, y^{k-2} + m^{k-2} \end{aligned}\right] \quad \ldots\ldots\ldots\ldots\ldots\ldots \quad \text{(A-10)}$$

Substitute (A-9) and (A-10) into (A-7),

$$(A^k M^k + B^k)\, y^k + C^k\, y^{k-1} = d^k - A^k\, m^k$$

Thus,

$$y^k = [A^k M^k + B^k]^{-1} \; [-C^k\, y^{k-1} + (d^k - A^k\, m^k)] \quad \ldots\ldots\ldots \quad \text{(A-11)}$$

Comparing (A-11) with the first equation of (A-10), we find

$$M^{k-1} = [A^k M^k + B^k]^{-1} \; [-C^k] \quad \ldots\ldots\ldots\ldots\ldots\ldots \quad \text{(A-12)}$$

$$m^{k-1} = [A^k M^k + B^k]^{-1} \; (d^k - A^k\, m^k) \quad \ldots\ldots\ldots\ldots\ldots\ldots \quad \text{(A-13)}$$

Using (A-4)

$$y^N = \begin{bmatrix} \overline{F} \\ \overline{G} \end{bmatrix} \quad \ldots\ldots\ldots\ldots\ldots\ldots\ldots\ldots\ldots\ldots \quad \text{(A-14)}$$

and from the first equation of (A-10) we obtain

$$M^{N-1} = 0 \quad \ldots\ldots\ldots\ldots\ldots\ldots\ldots\ldots\ldots\ldots \quad \text{(A-15)}$$

$$m^{N-1} = \begin{bmatrix} \overline{F} \\ \overline{G} \end{bmatrix} \quad \ldots\ldots\ldots\ldots\ldots\ldots\ldots\ldots\ldots\ldots \quad \text{(A-16)}$$

Now we can use (A-12) and (A-13) as recurrance formulas to obtain

$$\left.\begin{aligned} M^{N-2} &= \left[A^{N-1}\, M^{N-1} + B^{N-1}\right]^{-1} \left[-C^{N-1}\right] \\ m^{N-2} &= \left[A^{N-1}\, M^{N-1} + B^{N-1}\right]^{-1} \left[d^{N-1} - A^{N-1}\, m^{N-1}\right] \end{aligned}\right] \quad \ldots\ldots\ldots \quad \text{(A-17)}$$

$$\left.\begin{aligned} M^{N-3} &= \left[A^{N-2}\, M^{N-2} + B^{N-2}\right]^{-1} \left[-C^{N-2}\right] \\ m^{N-3} &= \left[A^{N-2}\, M^{N-2} + B^{N-2}\right]^{-1} \left[d^{N-2} - A^{N-2}\, m^{N-2}\right] \end{aligned}\right] \quad \ldots\ldots\ldots \quad \text{(A-18)}$$

and so on.

Having computed the M's and m's, we can calculate the solution by marching from $x = x_1$. Using boundary condition (A-3),

$$y^o = \begin{bmatrix} F \\ \\ G \end{bmatrix} \qquad \text{(A-19)}$$

the solution is

$$\left.\begin{aligned} y^1 &= M^o\, y^o + m^o \\ y^2 &= M^1\, y^1 + m^1 \end{aligned}\right\} \qquad \text{(A-20)}$$

and so on.

APPENDIX B - DIFFERENTIAL EQUATIONS FOR TIME-DEPENDENT SQUEEZE FILMS

If, in a gas bearing, one of the bearing surfaces is forced to vibrate normal to itself, the resulting oscillatory "squeeze-film" action can support a time-average load. This phenomenon is now well known, and a number of analyses have been published for various geometrical configurations. These analyses have been for "steady-state" squeeze films (in the sense of AC electrical terminology), there being no long-term transient in addition to the imposed high-frequency squeezing motion.

When long-term transients are present in the dynamic behavior of a squeeze-film bearing, the basic differential equation for the film is, of course, still applicable. However, numerical solution of this non-linear equation is impeded by the necessity of following the surface trajectories in detail through each cycle of the high-frequency squeeze action. To avoid excessive computer time consumption, it would be desirable to develop some form of differential equations in terms of "smoothed" dependent variables which exhibit only the long-term trends. Such a development is proposed in this note.

Basic Equations

The present work is an extension of that of Pan (Ref. 2), whose notation we adopt. Thus the basic Reynolds equation is written as:

$$\frac{\partial \rho h}{\partial t} + \nabla \cdot \left\{ \frac{\rho h \vec{V}}{2} - \frac{h^3}{12\mu} \rho \nabla p \right\} = 0 \quad \ldots\ldots\ldots\ldots\ldots\ldots \quad (B.1)$$

For a perfect gas: $p = \rho \mathcal{R} T(t)$ $\ldots\ldots\ldots\ldots\ldots\ldots\ldots\ldots$ (B.2)

(The bearing temperature may depend on time, but not position.) Then.

$$\frac{\partial \rho h}{\partial t} + \nabla \cdot \left\{ \frac{\rho h \vec{V}}{2} - \frac{h^3}{12\mu} \mathcal{R} T \rho \nabla \rho \right\} = 0 \quad \ldots\ldots\ldots\ldots\ldots\ldots \quad (B.3)$$

For air $\beta \sim T^{3/4}$ and, rather typically for perfect gases, T/μ depends only weakly on temperature. Accordingly, Eq. (B.3) is reduced to:

$$\frac{\partial \rho h}{\partial t} + \vec{V} \cdot \nabla \rho h = \frac{\mathcal{R} T}{12\mu} \nabla \cdot h^3 \rho \nabla \rho \quad \ldots\ldots\ldots\ldots\ldots\ldots \quad (B.4)$$

It is convenient to introduce a new dependent variable,

$$Q \equiv (\rho h)^2 \quad \ldots \quad (B.5)$$

and it is easily shown that Eq. (B.4) becomes:

$$\frac{1}{\sqrt{Q}}\left[\frac{\partial Q}{\partial t} + \frac{\vec{V}}{2} \cdot \nabla Q\right] = \frac{\mathcal{R}T}{12\mu} \nabla \cdot (h\nabla Q - 2Q\nabla h) \quad \ldots \quad (B.6)$$

The film thickness is hypothesized to have the form:

$$h = h_o (\vec{r},t) + \delta h (\vec{r},t) \cos(\omega t) \quad \ldots \quad (B.7)$$

Here h_o is the thickness corresponding to some long-term transient about which forced oscillations of amplitude δh and squeeze frequency "ω" take place.

The film response, in terms of Q, is hypothesized to have the form:

$$Q = Q_o (\vec{r},t) + \sum_n q_n (\vec{r},t) \cos\{n\omega t + \phi_n (\vec{r},t)\} \quad \ldots \quad (B.8)$$

In the last two equations, even as $\omega \to \infty$, the functions h_o, δh, Q_o, q_n and ϕ_n are presumed to be "smooth" in "t".

Smoothening of the Differential Equations

In the case of steady-state squeeze films, Pan (Ref. 2) has shown that, except near film edges, Q is smooth in spatial position "$\vec{r}$". It is anticipated that, with the same exception, Q will also be smooth in time "t". More specifically, there are two characteristic times associated with the film:

a) the squeeze period, $2\pi/\omega$

b) the "filling time", $\frac{12\mu(R/c)^2}{p_a}$

where "c" is a characteristic film thickness and "R" is a characteristic bearing dimension. Those functions whose fractional changes in one filling time are 0(1) are termed "smooth" in time.

An important consequence of the assumption of smoothness for "Q" is that, in the bearing interior,

$$q_n \to 0, \text{ all } n.^{*)} \text{ see footnote}$$

To smoothen Eq. (B.6), we integrate it from $t - \pi/\omega$ to $t + \pi/\omega$ and consider the order of magnitude of the various resultants when ω is very large.

The time-derivative term integrates directly to:

$$\sqrt{Q(t+\pi/\omega)} - \sqrt{Q(t-\pi/\omega)} =$$

$$\sqrt{Q_o(t+\pi/\omega) + \sum_n q_n(t+\pi/\omega) \cos\{n\omega(t-\pi/\omega) + \phi_n(t+\pi/\omega)\}}$$

$$-\sqrt{Q_o(t-\pi/\omega) + \sum_n q_n(t-\pi/\omega) \cos\{n\omega(t-\pi/\omega) + \phi_n(t-\pi/\omega)\}} = 0(\tfrac{1}{\omega}) \quad . . . \quad (B.9)$$

Here the average time derivative over one squeeze cycle is small because of the near-periodicity of all high-frequency components.

No time derivatives are involved in the second term $\vec{V} \cdot \nabla\sqrt{Q}$, so that integration yields directly

$$\vec{V} \cdot \nabla 0(\tfrac{1}{\omega}) \quad . . . . . \quad (B.10)$$

Footnote

T. Chiang observes that the assumption of spatial smoothness plus (B.8) suffices to give temporal smoothness in the interior. Thus, assume (B.8) to be valid and substitute into (B.6). The resulting equation is:

$$\frac{1}{\sqrt{Q}}\left[\frac{\partial Q_o}{\partial t} + \sum_n\left\{\frac{\partial q_n}{\partial t}\cos(n\omega t + \phi_n) - (n\omega + \frac{\partial \phi_n}{\partial t})q_n \sin(n\omega t + \phi_n)\right\} + \frac{\vec{V}}{2} \cdot \nabla Q\right]$$

$$= \frac{RT}{12\mu} \nabla \cdot (h\nabla Q - 2Q\nabla h)$$

$$\therefore q_n = 0\{\tfrac{1}{\omega}\} \times 0\{\text{Spatial derivatives}\}$$

But all spatial derivatives are 0(1), so $q_n \to 0$.

The actual magnitude of the term depends on the effect of spatial differentiation.

On the right-hand side of Eq. (B.6) we again conclude that all integrations give derivatives of terms of $0(\frac{1}{\omega})$, but it is desirable to ascertain the origins of the contributions. The process is aided by noting that:

$$\text{a)} \qquad \oint f(t) \begin{Bmatrix} \sin n\omega t \\ \cos n\omega t \end{Bmatrix} dt = 0(\frac{1}{\omega^2}) \qquad \ldots\ldots\ldots\ldots\ldots\ldots \quad (B.11)$$

for any smooth f(t)

$$\text{b)} \qquad \left.\begin{aligned} \oint \sin \omega t \cos n\omega t dt &= 0 \\ \oint \cos k\omega t \cos j\omega t dt &= \pi \delta_{kj} \end{aligned}\right\} \qquad \ldots\ldots\ldots\ldots\ldots \quad (B.12)$$

The appropriate rhs terms to retain are:

$$\nabla \cdot \left\{ h_o \nabla Q_o + \frac{\delta h}{2} \nabla(q_1 \cos\phi_1) - 2Q_o \nabla h_o - q_1 \cos\phi_1 \nabla \delta h \right\} \qquad \ldots\ldots\ldots \quad (B.13)$$

Since, in the interior of the bearing, the $q_n \to 0$, we recover Eq. (B.6) expressed in terms of zeroth-order functions. Namely,

<u>Inside Bearing:</u> $$\frac{1}{\sqrt{Q_o}} \left[\frac{\partial Q_o}{\partial t} + \frac{\vec{V}}{2} \cdot \nabla Q_o \right] =$$

$$\frac{\mathcal{R}T}{12\mu} \nabla \cdot (h_o \nabla Q_o - 2Q_o \nabla h_o) \qquad \ldots\ldots\ldots\ldots \quad (B.14)$$

This differential equation in terms of the smoothened variables Q_o and h_o is applicable to most of the bearing surface, and can, accordingly, be used to determine time-average load-carrying capacity. However, the applicable boundary conditions are, as yet, unknown.

Boundary Conditions for Smoothened Equation

To find appropriate boundary conditions, we recall that Pan (Ref.2) has shown that all inflow and outflow during a cycle at high squeeze frequency is confined to a very narrow edge strip of width $0(1/\sqrt{\omega})$. (See. Fig. B.1). On the outer edge of this strip (minus side)

$$\left.\begin{aligned} p_a &= \text{constant} \\ \rho_a &\equiv p_a/\mathcal{R}T(t) \\ h &= h_o + \delta h \cos\omega t \end{aligned}\right\} \qquad \ldots\ldots\ldots\ldots\ldots\ldots\ldots \qquad (B.15)$$

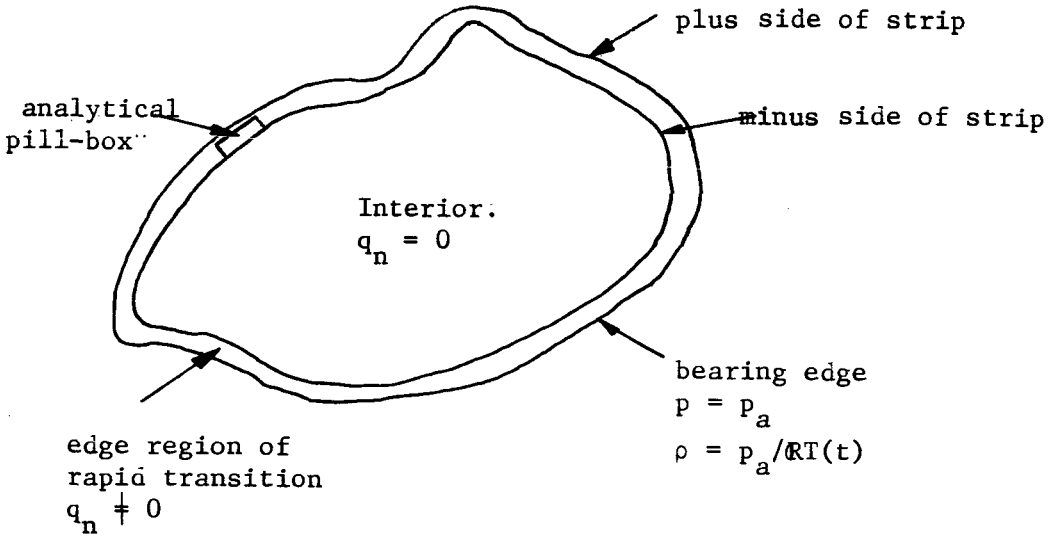

Fig. B.1 Plan View of Squeeze-Film Bearing of Arbitrary Shape

$$Q = (\rho_a h)^2 = \rho_a{}^2[h_o{}^2 + 2h_o\delta h \cos\omega t + (\delta h)^2 \cos^2\omega t]$$

$$= \rho_a{}^2\left[h_o^2 + \frac{(\delta h)^2}{2} + 2h_o\delta h \cos\omega t + \ldots\right] \qquad \ldots\ldots \qquad (B.16)$$

Therefore,

$$\left.\begin{aligned} Q_o &= \rho_a{}^2\left[h_o{}^2 + \frac{(\delta h)^2}{2}\right] \\ q_1 &= 2h_o\delta h\, \rho_a{}^2 \;;\; \cos\phi_1 = 1.0 \end{aligned}\right\} \qquad \ldots\ldots\ldots\ldots\ldots\ldots \qquad (B.17)$$

On the inner edge of the strip (plus side), all q_n vanish. It is clear then, that

$$\frac{\partial}{\partial n} q_1 = 0(\sqrt{\omega}) \quad \ldots\ldots\ldots\ldots\ldots\ldots\ldots \quad (B.18)$$

since Δq_1 across this strip is $0(1)$, and the strip width is $0(1/\sqrt{\omega})$.

To proceed further, consider the full time-averaged equation consisting of the averaged time-derivative (B.9), the averaged convective term (B.10) and the averaged divergence term (B.13).

Take a pill-box within the edge region, as shown in Fig. B.1. Let its bottom border the bearing interior, and let its top lie somewhere towards the true bearing edge. Integrate the total DE over the pill-box volume, which is $0(1/\sqrt{\omega})$. The results obtained are shown below.

(B.9) $\downarrow$ $0\left(\frac{1}{\omega^{3/2}}\right)$ (B.10) $\downarrow$ $0\left(\frac{1}{\omega}\right)$ (B.13)

$$h_o \frac{\partial Q_o}{\partial n} + \frac{\delta h}{2} \frac{\partial}{\partial n} (q_1 \cos\phi_1)$$
$$-2Q_o \frac{\partial h_o}{\partial n} - q_1 \cos\phi_1 \frac{\partial \delta h}{\partial n}$$
$$-h_o^- \frac{\partial Q_o^-}{\partial n} + 2Q_o^- \frac{\partial h_o^-}{\partial n} \quad \ldots\ldots \quad (B.19)$$

Now the functions h_o and δh are spatially smooth everywhere, and the derivative of Q_o is certainly small bordering the bearing interior. Hence.

$$h_o \frac{\partial Q_o}{\partial n} + \frac{\partial h}{2} \frac{\partial}{\partial n} (q_1 \cos\phi_1) \overset{\sim}{=} 0 \quad \ldots\ldots\ldots\ldots\ldots\ldots \quad (B.20)$$

although, individually, the terms may be large. A second integration across the entire edge strip gives (treating h_o and δh as constant):

$$h_o Q_o^+ + \frac{\delta h}{2} q_1^+ \cos\phi_1^+ = h_o Q_o^- \quad \ldots\ldots\ldots\ldots\ldots\ldots \quad (B.21)$$

Reference to Eq. (B.17) now shows that:

$$Q_o^- = \rho_a{}^2 h_o{}^2 \left[1 + \frac{3}{2} \left(\frac{\delta h}{h_o}\right)^2\right] \quad \ldots\ldots\ldots\ldots\ldots\ldots\ldots\ldots \quad (B.22)$$

At a given time all quantities on the right hand side of Eq. (B.22) are known and it supplies the boundary condition for DE (B. 14).

Incorporation of Bearing Dynamics

The average local pressure during a squeeze cycle is given by:

$$p_{av} = p_o = \oint \frac{pdt}{(2\pi/\omega)} = \frac{\omega}{2\pi} \oint \frac{\sqrt{Q}}{h} \mathcal{R}Tdt \quad \ldots\ldots\ldots\ldots \quad (B.23)$$

Exclusive of the edge region:

$$Q = Q_o(t) \quad \ldots\ldots\ldots\ldots\ldots\ldots\ldots\ldots \quad (B.24)$$

But asymptotically in "ω", T, Q_o, h_o, δh can be treated as constant during one squeeze cycle

$$\therefore p_o = \frac{\omega}{2\pi} \mathcal{R}T \sqrt{Q_o} \oint \frac{dt}{h} \quad \ldots\ldots\ldots\ldots\ldots\ldots \quad (B.25)$$

Or:

$$p_o = \mathcal{R}T \frac{\sqrt{Q_o}}{h_o^2 - (\delta h)^2} \quad \ldots\ldots\ldots\ldots\ldots\ldots\ldots\ldots \quad (B.26)$$

In this last expression, T, Q_o, h_o, δh, can be regarded as time-dependent despite the fact that they were treated as constants during one period of the squeeze cycle.

It is now entirely possible to investigate some cases of bearing dynamics. For example, consider the squeeze-film suspension of a mass, M, as shown in Fig. 4.1. Let the instantaneous elevation of the vibrating plate be:

$$y_1 = -\delta h \cos\omega t \quad \ldots\ldots\ldots\ldots\ldots\ldots\ldots\ldots \quad (B.27)$$

and the instantaneous elevation of the lower surface of mass M be:

$$y_2(t) \quad \ldots\ldots\ldots\ldots\ldots\ldots\ldots\ldots \quad (B.28)$$

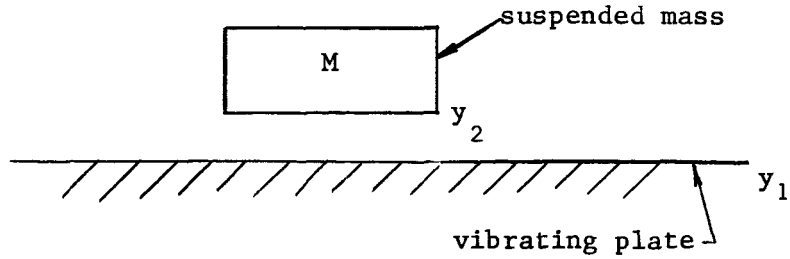

Fig. B.2 - Elementary Dynamical Problem with Squeeze Film

Then $h = y_2(t) + \delta h \cos\omega t$ . . . . . (B.29)

or: $h_o(t) = y_2(t)$ . . . . . (B.30)

Let the film temperature be constant. Then:

$$M \frac{d^2 h_o}{dt^2} = A \left[\frac{\mathcal{R}T \sqrt{Q_o}}{h_o^2 - (\delta h)^2} - p_a \right] - MG \quad . . . . . \quad (B.31)$$

where "A" is the bearing face area. Initial conditions for h_o and dh_o/dt must be given.

The accompanying DE for Q_o is obtained from (B.14). Thus:

$$\frac{1}{\sqrt{Q_o}} \frac{\partial Q_o}{\partial t} = \frac{\mathcal{R}Th_o}{12\mu} \nabla^2 Q_o \quad . . . . . \quad (B.32)$$

with the boundary condition from (B.22)

$$Q_o = \left(\frac{P_a}{\mathcal{R}T}\right)^2 \left\{ h_o^2 + \frac{3}{2} (\delta h)^2 \right\} \quad . . . . . \quad (B.33)$$

Some initial distribution of "ρ" throughout the bearing film must also be given. The mathematical problem for following the mass motion and average film history is then completely posed.

Nomenclature for Appendix B

A	bearing face area
c	characteristic film thickness
h	film thickness
h_o	long-term transient film thickness
δh	amplitude of squeeze motion
M	bearing mass
p	pressure
Q	$(\rho h)^2$
Q_o, q_n	defined in Eq. (B.8)
r	space coordinate
R	characteristic bearing dimension
$\mathcal{R}$	gas constant
t	time
T	temperature
y_1, y_2	displacements (see Fig. B.2)
ρ	density
ϕ_n	phase angle defined in Eq. (B.8)
ω	squeeze frequency (in this appendix)

REFERENCES

1. Pan, C.H.T., "Gas Lubricated Spherical Bearings", Trans. ASME, J. of Basic Engineering, Vol. 85, Series D, No. 2, p. 311, June 1963.
2. Pan, C.H.T., "On Asymptotic Analysis of Gaseous Squeeze-Film Bearings", MTI Technical Report 65TR20, April, 1965, also to be published in Trans. ASME.
3. Pan, C.H.T., "Spectral Analysis of Gas Bearing Systems for Stability Studies", Presented at the Ninth Midwestern Mechanics Conference, University of Wisconsin, Madison, Wis., August, 1965.
4. Chiang, T., Malanoski, S.B. and Pan, C.H.T., "Spherical Squeeze-Film Hybrid Bearing with Small Steady-State Radial Displacement", MTI Report 65TR30, November, 1965.
5. Pan, C.H.T., and Malanoski, S.B., Discussion of "On the Behavior of Gas Lubricated Journal Bearings Subjected to Sinusoidally Time-Varying Loads", by J.S. Ausman, Trans. ASME, J. of Basic Engineering, Vol. 87, Series D, No. 3, p. 599, September 1965.
6. Peirce, B.O., "A Short Table of Integrals", Ginn and Company, 1956.
7. Castelli, V. and Pirvics, J., "Equilibrium Characteristics of Axial-Groove Gas Lubricated Bearings,"ASLE-ASME Lubrication Conference, San Francisco, California, October, 1965.

NOMENCLATURE

C	bearing clearance
D	bearing diameter
f_1, f_2, f_3	defined in Eq. (2.39)
f_x, f_y	defined in Eq. (5.9)
F_x, F_y	components of dynamic bearing forces in a plane perpendicular to the z-axis
F_z	axial dynamic bearing force
$g_o, g_1, \cdots g_5$	defined in Eq. (2.21)
g_z	defined in Eq. (2.21)
h_o, h_1	defined in Eq. (2.23)
H	normalized film thickness
H_∞	defined in Eq. (2.9)
i	$\sqrt{-1}$
$K_R^{(j)}, K_T^{(j)}$	defined in Eq. (3.16) and (3.17)
m	dimensionless mass defined in (5.2)
m_o	critical dimensionless mass
M	journal mass
M_o	critical journal mass
p	pressure
p_a	ambient pressure
P	p/p_a
R	bearing radius
Re { }	real part of { }
t	time
t_r, t_z	reference times
T	νt
T_r, T_z	defined in Eq. (2.20a)
u_j, v_j	real and imaginary parts of g_j, $j=1,2, \ldots 5$
U_z, V_z	axial dynamic stiffness and damping

x, y	coordinates in Fig. 2
z	coordinate in the axial direction
Z_{xx}, Z_{xy}, Z_{yx}, Z_{yy}	defined in (3.18) and (3.19)
δ_x^* , δ_y^*	amplitudes of vibration in the respective directions
δ_x, δ_y	δ_x^*/C, δ_y^*/C
δ_z^*	amplitude of axial vibration
δ_z	δ_z^*/C
ε^*	excursion amplitude
ε	excursion ratio, ε^*/C
η_r^*, η_z^*	radial and axial displacement
η_r, η_z	η_r^*/C, η_z^*/C
θ	meridional angle of spherical coordinates
Λ	compressibility number, defined in (2.7)
Λ_1, Λ_2	defined in (2.28)
μ	viscosity
ν	vibration frequency
ν_r, ν_z	radial and axial vibration frequencies
ζ	vibration number, defined in (2.7)
ζ_z	axial vibration number, defined in (2.28)
σ	squeeze number, defined in (2.7)
τ	Ωt
Ψ	PH
Ψ_∞	asymptotic solution of Ψ for $\sigma \to \infty$

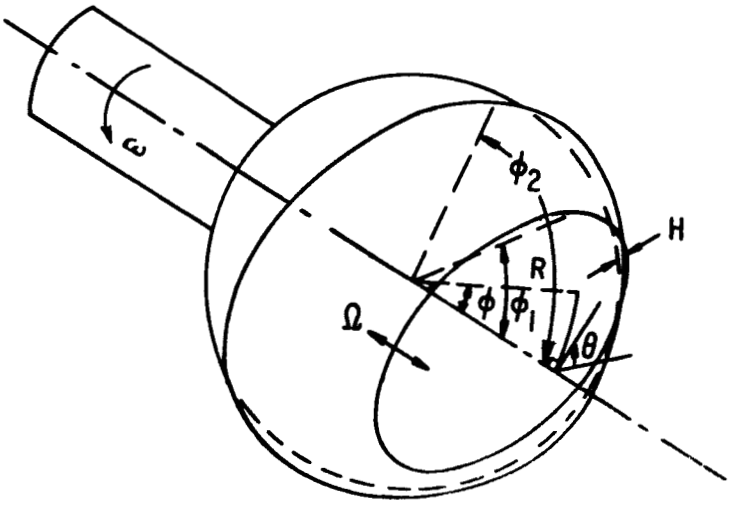

Fig. 1 Spherical Squeeze-Film Bearing

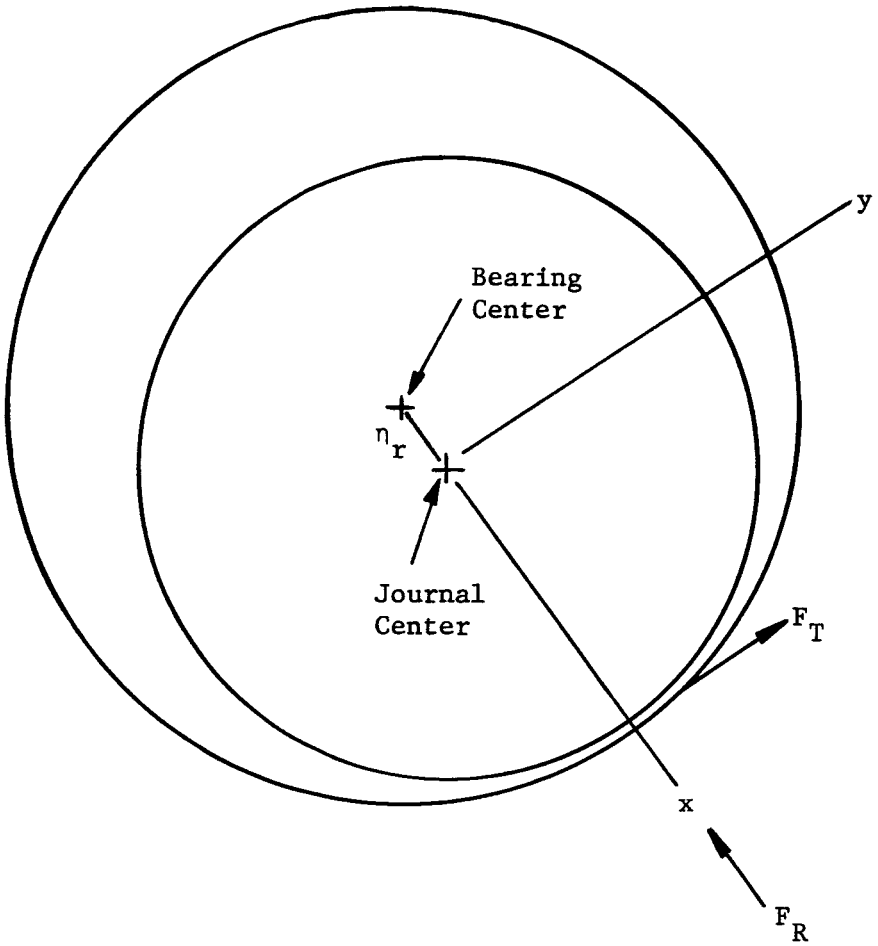

Fig. 2 Diagram illustrating x and y coordinates in a plane perpendicular to the z-axis

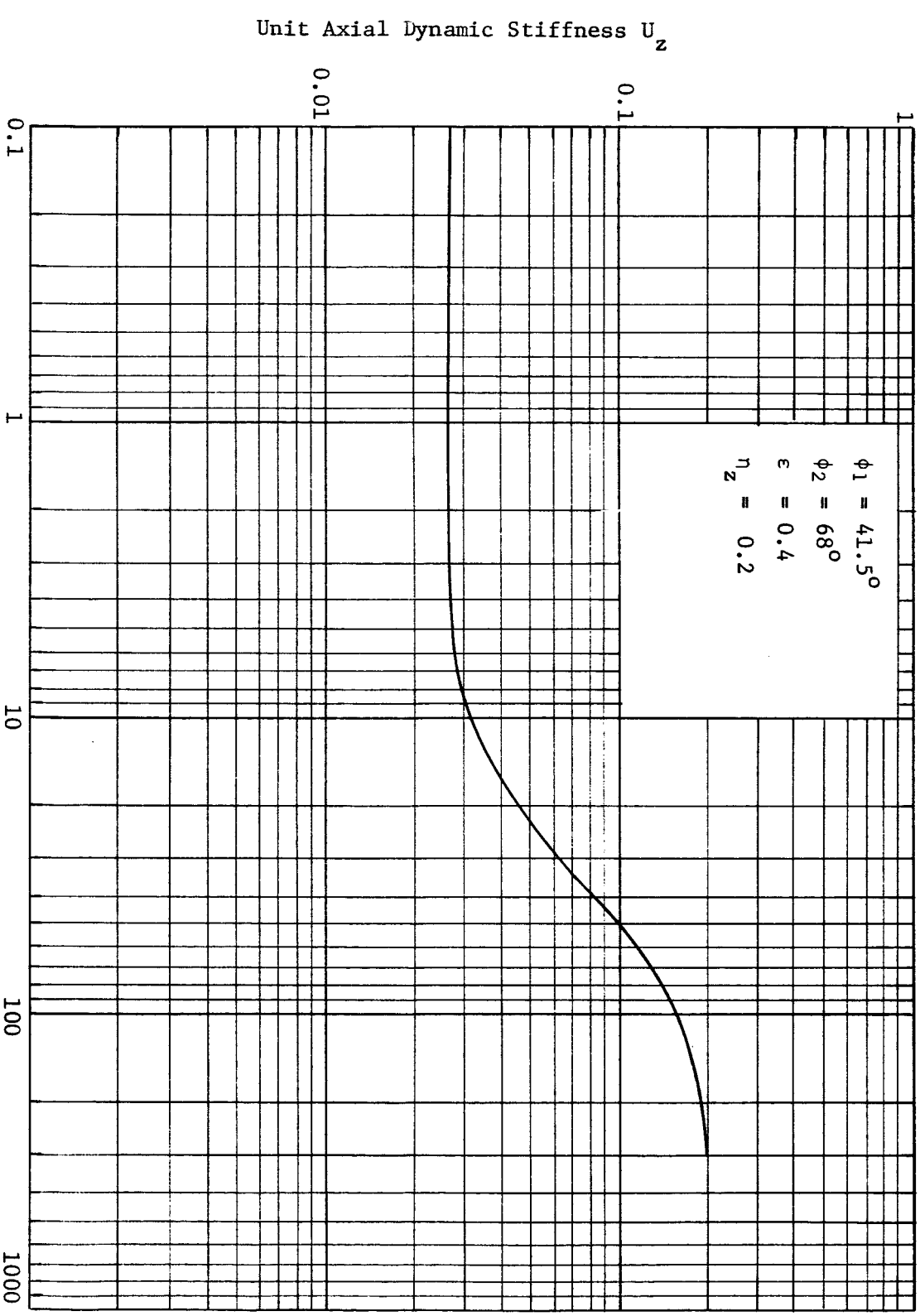

Fig. 3 Unit Axial Dynamic Stiffness U_z against ζ_z

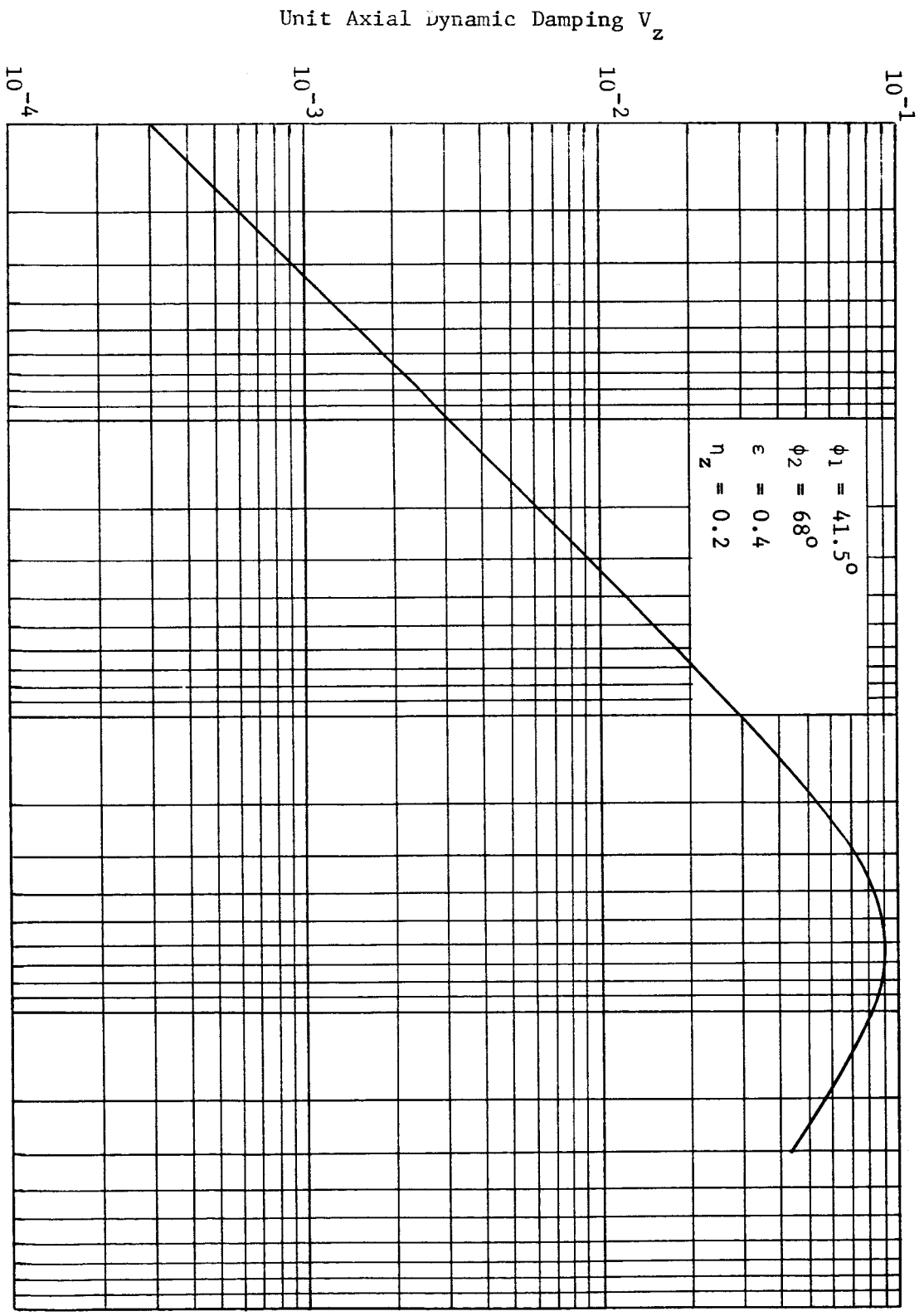

Fig. 4 Unit Axial Dynamic Damping V_z against ζ_z.

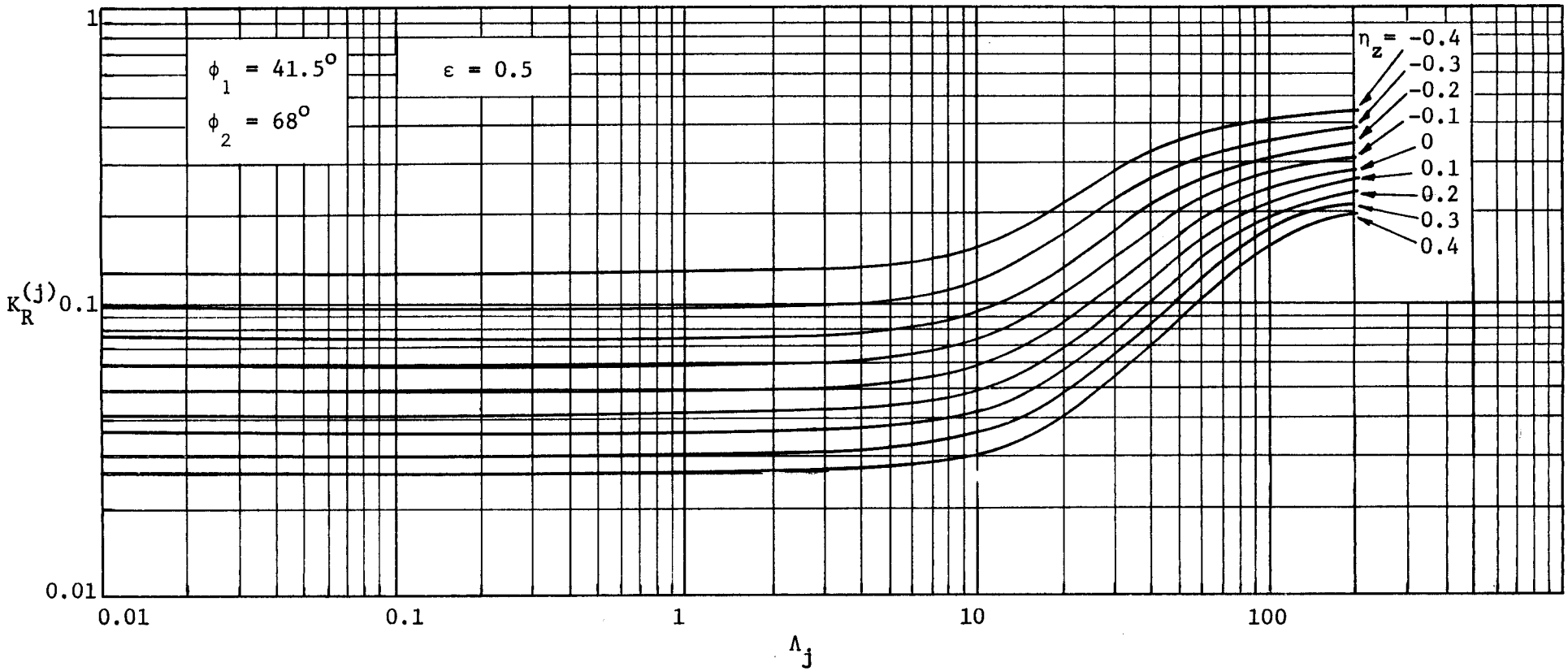

Fig. 5 $K_R^{(j)}$ vs. Λ_j for various axial displacement ratio

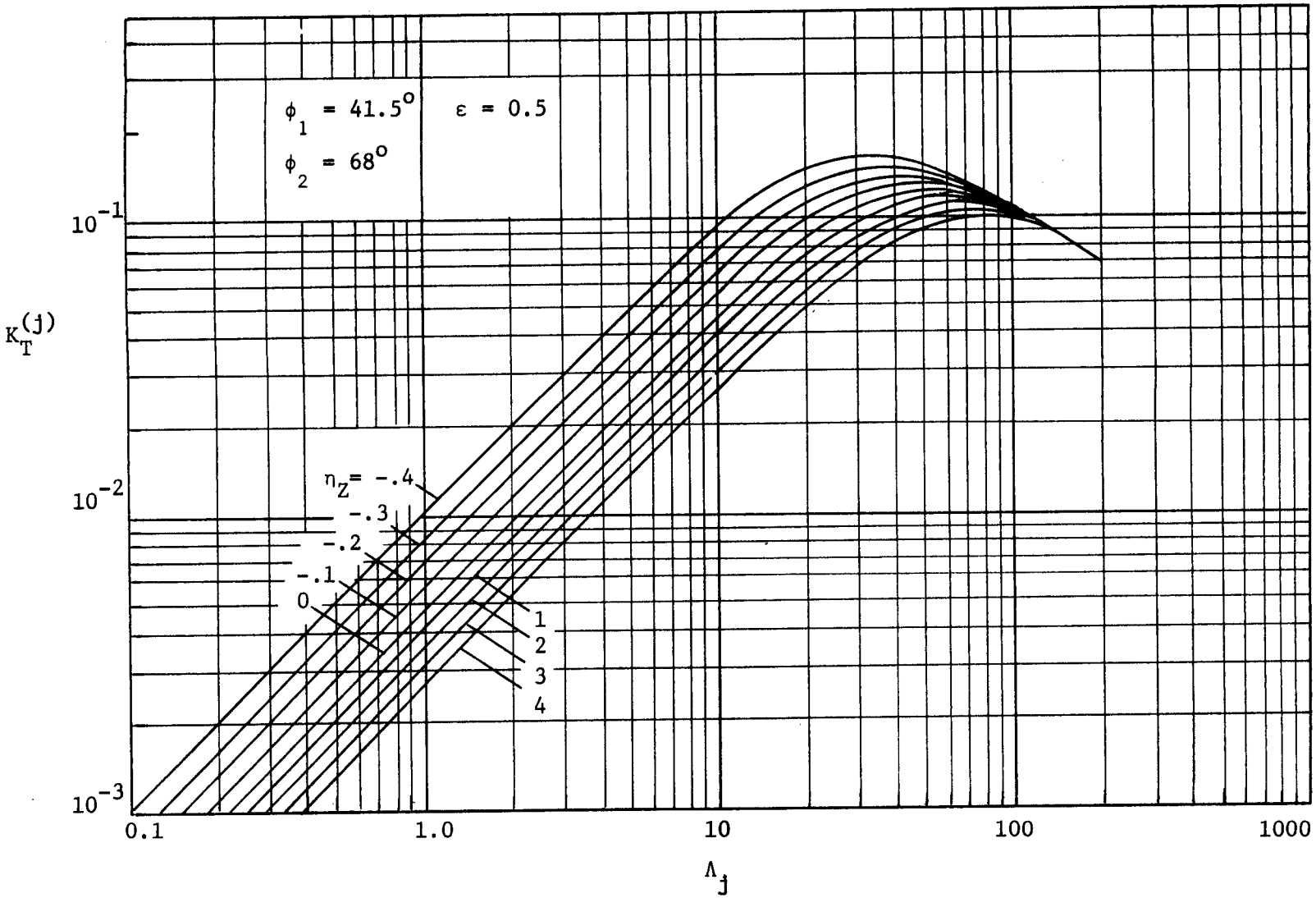

Fig. 6 $K_T^{(j)}$ vs. Λ_j for various axial displacement ratio

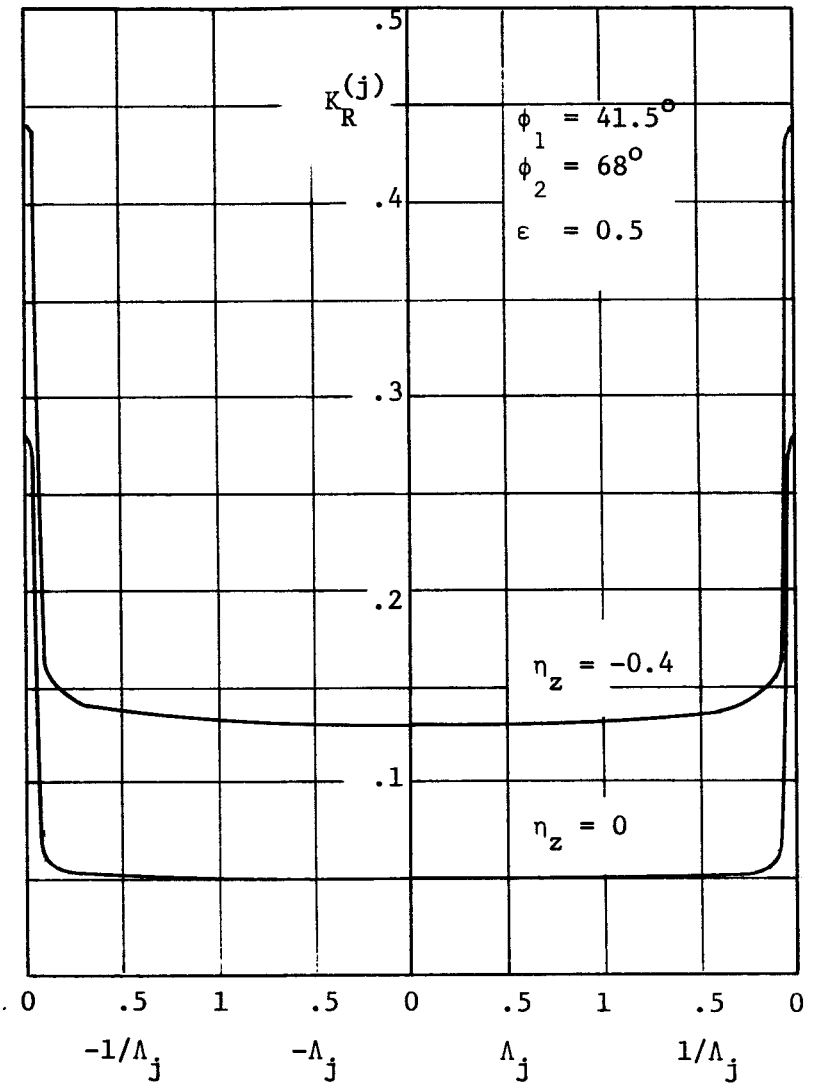

Fig. 7 $K_R^{(j)}$ against Λ_j

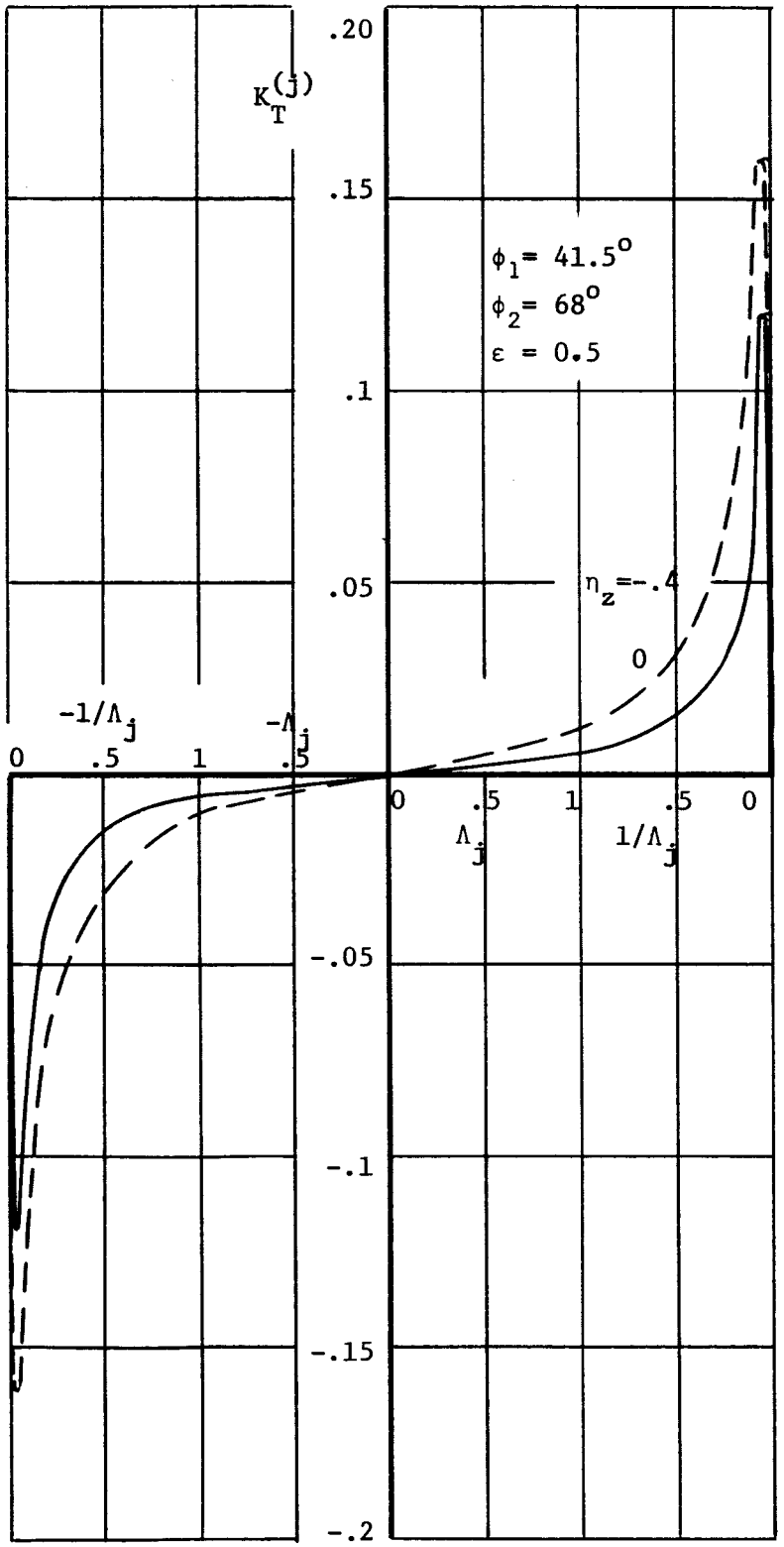

Fig. 8 $K_T^{(j)}$ against Λ_j